NASA Technical Memorandum 101330

Three-Dimensional Elliptic Grid Generation Technique With Application to Turbomachinery Cascades

(NASA-TM-101330) THREE-DIMENSIONAL ELLIPTIC GRID GENERATION TECHNIQUE WITH APPLICATION TO TURBOMACHINERY CASCADES (NASA) 20 p CSCL 20D

N88-30078

Unclas G3/34 0161725

S.C. Chen
Sverdrup Technology, Inc.
NASA Lewis Research Center Group
Cleveland, Ohio

and

J.R. Schwab
National Aeronautics and Space Administration
Lewis Research Center
Cleveland, Ohio

August 1988

NASA

THREE-DIMENSIONAL ELLIPTIC GRID GENERATION TECHNIQUE WITH APPLICATION TO TURBOMACHINERY CASCADES

S. C. Chen
Sverdrup Technology, Inc.
NASA Lewis Research Center Group
Cleveland, Ohio 44135

and

J. R. Schwab
National Aeronautics and Space Administration
Lewis Research Center
Cleveland, Ohio 44135

SUMMARY

This report describes a numerical method for generating three-dimensional grids for turbomachinery computational fluid dynamics codes. The basic method is general and involves the solution of a quasi-linear elliptic partial differential equation via pointwise relaxation with a local relaxation factor. It allows specification of the grid point distribution on the boundary surfaces, the grid spacing off the boundary surfaces, and the grid orthogonality at the boundary surfaces. It includes adaptive mechanisms to improve smoothness, orthogonality, and flow resolution in the grid interior. A geometry preprocessor constructs the grid point distributions on the boundary surfaces for general turbomachinery cascades. Representative results are shown for a C-grid and an H-grid for a turbine rotor. Two appendices serve as user's manuals for the basic solver and the geometry preprocessor.

INTRODUCTION

Three-dimensional computational fluid dynamics codes require computational grids with suitable resolution, smoothness, and orthogonality. High grid resolution allows complex flow physics to be modelled near shocks and in shear layers. Smoothness of the metric data prevents the flow solution from being dominated by truncation error in the metric coefficients. Grid orthogonality at the boundaries simplifies and improves the accuracy of any boundary condition involving normal gradients.

The above qualities are especially difficult to maintain for realistic turbomachinery geometries. Modern three-dimensional designs comprise tapered, twisted, leaned, and bowed blade shapes within contoured endwalls to tailor secondary flows. Centrifugal compressors and radial turbines involve simultaneous flow turning in the meridional and blade-to-blade planes. The periodicity condition within blade rows poses an additional unique problem.

Current grid generation technology is fairly well developed for general two-dimensional turbomachine cascade geometries. Conformal mapping, algebraic interpolation, and partial differential equation methods are all used successfully. The general three-dimensional geometry represented by a realistic turbomachine cascade has unique requirements for a body-fitted grid that have not been met with current technology.

This report describes a numerical method for generating three-dimensional grids for turbomachinery computational fluid dynamics codes. The basic method is general and involves the solution of a quasi-linear elliptic partial differential equation via pointwise successive over-relaxation with a local relaxation factor. The governing equation contains forcing functions that depend upon the boundary point distribution and the boundary surface gradient. The method allows specification of the grid point distribution on the boundary surfaces, the grid spacing off the boundary surfaces, and the grid orthogonality at the boundary surfaces. It includes adaptive mechanisms to improve smoothness, orthogonality, and flow resolution in the grid interior. A geometry preprocessor constructs the grid point distributions on the boundary surfaces for general turbomachinery cascades. It utilizes a two-dimensional version of the basic solver and algebraic interpolation to form the boundary distributions for the three-dimensional basic solver.

This report includes a description of the coordinate system , a discussion of the mathematical formulation of the method, and some representative results. Two appendices serve as the user's manuals for the geometry preprocessor and the basic solver.

COORDINATE SYSTEM

The partial differential equations for computational fluid dynamics codes are usually described with reference to a generalized coordinate system to simplify the implementation and make it independent of any specific geometry. The function of a grid generation system is to generate an ordered distribution of points in physical space to align with some body-conforming generalized coordinate system in computational space. Physical space is described with reference to a cartesian coordinate system for the grid generation technique described in this report. Each boundary surface segment in physical space must coincide with a boundary surface segment in computational space.

Three types of generalized body-conforming coordinate systems are commonly used for turbomachinery cascades: C-grid, H-grid, and O-grid. The grid generation technique described in this report can produce C-grids and H-grids.

Figure 1(a) shows a C-grid about a generic blade shape in the cartesian (x_1, x_2, x_3) coordinate system in physical space. The inlet surface is A1-A2-A2′-A1′ and the outlet surface is B1-B2-B2′-B1′. The hub endwall surface is A1′-B1′-B2′-A2′ and the shroud endwall surface is A1-B1-B2-A2. The periodic surfaces are A1-B1-B1′-A1′ and A2-B2-B2′-A2′. The blade surface is the wrapped D-E-D-D′-E′-D′ surface. Surface C-D-D′-C′ represents a branch cut from the wrapped blade surface to the outlet surface. Figure 1(b) shows the C-grid in the generalized (ξ_1, ξ_2, ξ_3) coordinate system in computational space.

Figure 2(a) shows an H-grid between two generic blade shapes in the cartesian (x_1, x_2, x_3) coordinate system in physical space. The inlet surface is A1-A2-A2′-A1′ and the outlet surface is B1-B2-B2′-B1′. The hub endwall is A1′-B1′-B2′-A2′ and the shroud endwall surface is A1-B1-B2-A2. The periodic surfaces are A1-C1-C1′-A1′, A2-C2-C2′-A2′, D1-B1-B1′-D1′, and D2-B2-B2′-D2′. The blade surfaces are C1-D1-D1′-C1′ and C2-D2-D2′-C2′. Figure 2(b) shows the H-grid in the generalized (ξ_1, ξ_2, ξ_3) coordinate system in computational space.

MATHEMATICAL FORMULATION

The quasi-linear elliptic governing equation is taken from reference 1 as

$$\sum_{i=1}^{3}\sum_{j=1}^{3} g^{ij} \frac{\partial^2 \tilde{x}}{\partial \xi_i \partial \xi_j} + \sum_{k=1}^{3} g^{kk} P_k \frac{\partial \tilde{x}}{\partial \xi_k} = 0. \tag{1}$$

The metric tensor components g^{ij} and g^{kk} in equation (1) are defined as

$$g^{ij} = \tilde{a}^i \cdot \tilde{a}^j \tag{2}$$

where

$$\tilde{a}^i = \tilde{a}_j \times \tilde{a}_k \;/\; \sqrt{g} \qquad i, j, k \text{ cyclic}$$
$$\sqrt{g} = \tilde{a}_1 \cdot (\tilde{a}_2 \times \tilde{a}_3)$$
$$\tilde{a}_i = \frac{\partial \tilde{x}}{\partial \xi_i}.$$

The $\tilde{x}$ in equation (1) represents the position vector in physical space with cartesian (x_1, x_2, x_3) components. The P_k are the forcing functions specified by the user. They represent one-dimensional stretching in each coordinate direction. Values of the forcing functions on the boundaries are determined by specification of the boundary point distribution and the boundary surface gradient. Values of the forcing functions in the interior are determined by interpolation of the values on the boundaries.

Equation (1) can be rewritten using matrix notation as

$$\mathbf{A} + \mathbf{B}\,\mathbf{P} = \mathbf{0} \tag{3}$$

where

$$\mathbf{A} = \begin{pmatrix} g^{11}\frac{\partial^2\tilde{x}}{\partial\xi_1^2} & g^{12}\frac{\partial^2\tilde{x}}{\partial\xi_1\partial\xi_2} & g^{13}\frac{\partial^2\tilde{x}}{\partial\xi_1\partial\xi_3} \\ g^{21}\frac{\partial^2\tilde{x}}{\partial\xi_2\partial\xi_1} & g^{22}\frac{\partial^2\tilde{x}}{\partial\xi_2^2} & g^{23}\frac{\partial^2\tilde{x}}{\partial\xi_2\partial\xi_3} \\ g^{31}\frac{\partial^2\tilde{x}}{\partial\xi_3\partial\xi_1} & g^{32}\frac{\partial^2\tilde{x}}{\partial\xi_3\partial\xi_2} & g^{33}\frac{\partial^2\tilde{x}}{\partial\xi_3^2} \end{pmatrix}$$

$$\mathbf{B} = \begin{pmatrix} g^{11}\frac{\partial^2\tilde{x}}{\partial\xi_1^2} & 0 & 0 \\ 0 & g^{22}\frac{\partial^2\tilde{x}}{\partial\xi_2^2} & 0 \\ 0 & 0 & g^{33}\frac{\partial^2\tilde{x}}{\partial\xi_3^2} \end{pmatrix}$$

$$\mathbf{P} = \begin{pmatrix} P_1 \\ P_2 \\ P_3 \end{pmatrix}$$

Equation (3) can be solved for P_k on the boundaries as

$$\mathbf{P_0} = -\mathbf{B_0^{-1}}\,\mathbf{A_0} \tag{4}$$

where the subscript "0" indicates values on the boundary. Tangential derivatives for terms on the right hand side of equation (4) are determined by applying standard difference formulas to the prescribed boundary point distribution on the surface. Normal derivatives are determined by specifying the first normal derivative equal to the desired spacing off the boundary and using the approximation

$$\frac{\partial^2\tilde{x}_0}{\partial n^2} = \frac{2(\tilde{x}_1 - \tilde{x}_0)}{(\Delta n)^2} - \frac{2}{\Delta n}\frac{\partial\tilde{x}_0}{\partial n} \tag{5}$$

where n indicates the normal direction, the subscript "0" indicates values on the boundary, and the subscript "1" indicates values one point away from the boundary.

Once the boundary values are known, the interior values of P_k can be determined using

$$P_k(\xi_1,\xi_2,\xi_3) = \sum_{l=1}^{3} P_{0_{k,l,1}}\,(1+\alpha_{k,l,1})\,\gamma_{k,l,1} + \sum_{l=1}^{3} P_{0_{k,l,2}}\,(1+\alpha_{k,l,2})\,\gamma_{k,l,2} \tag{6}$$

where

$$\begin{aligned}
\alpha_{k,l,1} &= C_{\alpha_{k,l,2}}\,(\xi_l - \xi_{l_{min}})/(\xi_{l_{max}} - \xi_{l_{min}}) \\
\alpha_{k,l,2} &= C_{\alpha_{k,l,2}}\,(\xi_{l_{max}} - \xi_l)/(\xi_{l_{max}} - \xi_{l_{min}}) \\
\beta_{k,l,1} &= [(\xi_{l_{max}} - \xi_{l_{min}})/(\xi_l - \xi_{l_{min}})]^{C_{\beta_{l,1}}} \\
\beta_{k,l,2} &= [(\xi_{l_{max}} - \xi_{l_{min}})/(\xi_{l_{max}} - \xi_l)]^{C_{\beta_{l,2}}} \\
\gamma_{k,l,1} &= \beta_{k,l,1}\Big/\left(\sum_{m=1}^{3}\beta_{k,l,1} + \sum_{m=1}^{3}\beta_{k,l,2}\right) \\
\gamma_{k,l,2} &= \beta_{k,l,2}\Big/\left(\sum_{m=1}^{3}\beta_{k,l,1} + \sum_{m=1}^{3}\beta_{k,l,2}\right).
\end{aligned}$$

The value of $P_{0_{k,l,1}}$ represents the k-th component of the $\mathbf{P_0}$ vector on the minimum boundary surface in the l-th direction. The value of $P_{0_{k,l,2}}$ represents the k-th component of the $\mathbf{P_0}$ vector on the maximum boundary surface in the l-th direction. The functions α, β, and γ have subscript notation similar to that of P_0. The α function represents linear extrapolation from a controlled boundary using a constant factor C_α.

The γ function represents the combined effect of the β functions, which represent power-law factorization with constant exponent C_β to control the depth of influence away from a controlled boundary.

The values of the forcing functions can be modified for improved smoothness by using

$$P'_k = \theta \; P_k \tag{7}$$

where

$$\theta = 1 - \tanh(C_{\theta_1}(1 - \sigma^{C_{\theta_2}}))$$
$$\sigma = J/(\|l_1\| \cdot \|l_2\| \cdot \|l_3\|) .$$

The constants C_{θ_1} and C_{θ_2} define the rate and order of the adaptation. The variable σ is a measure of the shear of the grid, with J representing the Jacobian and l_1, l_2, l_3 representing the grid cell lengths in each direction.

A measure of the local orthogonality of the grid can be defined as

$$\phi = \sigma^{C_\phi}/J. \tag{8}$$

The constant exponent C_ϕ defines the order of the adaptation. A one-dimensional variational form of equation (8) can then be written as

$$\phi'_k = \frac{\delta_k(J)}{J} - C_\phi \frac{\delta_k(\sigma)}{\sigma}. \tag{9}$$

If a flow variable gradient E is computed by the flow solver such that $E \geq 0$, a measure of the local flow resolution can be defined as

$$\psi = J(1 + E). \tag{10}$$

A one-dimensional variational form of equation (10) can then be written as

$$\psi'_k = \frac{\delta_k(J)}{J} - \frac{\delta_k(E)}{1 + E}. \tag{11}$$

The values of the forcing functions can be modified for improved local orthogonality and flow resolution using

$$\begin{aligned} P'_k &= (1 + \lambda_k)P_k \qquad F_k \cdot P_k > 0 \\ P'_k &= (1 - \lambda_k)P_k \qquad F_k \cdot P_k < 0 \end{aligned} \tag{12}$$

where

$$\lambda_k = C_{\lambda_1} \tanh(C_{\lambda_2}|F_k|^{C_{\lambda_3}})$$
$$F_k = (W_\phi \phi'_k + W_\psi \psi'_k)/(W_\phi + W_\psi)$$

with the constants C_{λ_1}, C_{λ_2}, and C_{λ_3} determining the range, rate, and order of the adaptation. The variable F represents a weighted combination of the skewness and flow error variations, with W_ϕ and W_ψ as the respective weighting constants.

These adaptive adjustments to the forcing functions can be employed in an accumulative or a non-accumulative manner. Under the accumulative method, the adjustments are lagged, but the forcing functions always satisfy the physical constraints. Under the non-accumulative method, the adjustments are immediate, but they are limited by the range and rate constants.

The following sequence is iterated until convergence is attained:

1. Solve the governing equation with current forcing functions using pointwise relaxation with a local relaxation factor for stability.
2. Evaluate the second normal derivatives on the boundary surfaces.
3. Evaluate the forcing functions on the boundary surfaces.

4. Evaluate the forcing functions in the interior by interpolation.
5. Adjust the forcing functions for adaptive smoothness, orthogonality, and flow resolution.

RESULTS

Figure 3 shows a three-dimensional C-grid for a turbine rotor. The grid comprises 101 points in the ξ_1 direction around the blade, 16 points in the ξ_2 direction away from the blade, and 15 points in the ξ_3 direction from hub to tip. The grid was truncated in the ξ_1 direction and thinned in the ξ_2 direction to improve the appearance of the figure. The spacing at the solid surfaces was specified as 0.1 relative to the uniform unit spacing. Default values were used for all other variables. This grid required approximately 1200 seconds of Cray X-MP computing time for 600 iterations.

Figure 4 shows a three-dimensional H-grid for the same turbine rotor as Figure 3. The grid comprises 61 points in the streamwise ξ_1 direction, 31 points in the pitchwise ξ_2 direction, and 15 points in the radial ξ_3 direction. The grid was thinned in the ξ_2 direction to improve the appearance of the figure. The spacing at the solid surfaces was specified as 0.1 relative to the uniform unit spacing. Default values were used for all other variables. This grid required approximately 1400 seconds of Cray X-MP computing time for 600 iterations.

CONCLUDING REMARKS

A general numerical method for generating three-dimensional grids was developed and implemented along with a geometry preprocessor for turbomachinery cascades. Results were shown for a C-grid and an H-grid for a turbine rotor. The method includes an adaptive mechanism for improved flow resolution when coupled with a flow solver, but this was not demonstrated. Since the basic method is completely general, additional preprocessors for other physical geometries could be developed to extend the application of this grid generation method.

APPENDIX A

USER'S MANUAL FOR BASIC SOLVER

The basic solver is coded in FORTRAN IV as program GRID3D with 34 subprograms. The nonstandard PARAMETER statement is used to facilitate dimensioning of arrays, while the nonstandard NAMELIST feature is used for quasi-free-format input. Figure 5 shows a flow chart of the program.

Input to the basic solver comprises three namelists read on unit 5 and the initial grid binary file read on unit 10. The type (REAL or INTEGER) of each variable follows standard FORTRAN convention. The I, J, and K indices correspond to the ξ_1, ξ_2, and ξ_3 directions, respectively.

Namelist SYSTEM

ISYS	= 1	Solve governing equation as a Laplacian system without forcing functions (default). This option produces a grid that tends toward uniform spacing away from curved boundaries, but produces smaller spacing near convex boundaries and larger spacing near concave boundaries.
	= 2	Solve governing equation as a Poission system with forcing functions. This option allows specificaton of spacing and orthogonality at the boundaries.
INTERP	= 1	Run three-dimensional interpolation as initial guess (default). This option is used when the geometry preprocessor is employed to generate the initial grid binary file without interior values.
	= 0	Bypass three-dimensional interpolation. This option is used when a complete initial grid binary file is imported from another grid generator.
ICHECK	= 1	Check boundary structures for grid folding and write report on unit 20.
	= 0	Bypass boundary structure check (default).
ICONT	= 0	Terminate operation if boundary structure grid folding is detected.
	= 1	Continue operation (default).
ITMAX		Maximum number of overall iterations (default = 100).
LREFI	= 1	Establish a reference length scale for spacing off the I = 1 and I = IMAX surfaces based upon the unit length in the J-direction for each K-layer at the I = 1 surface. The unit length is defined as (total length)/(number of points - 1).
	= 2	Establish a reference length scale for spacing off the I = 1 and I = IMAX surfaces based upon the local unit length in the J-direction. The unit length is defined as (total length)/(number of points - 1).
	= 3	Establish a reference length scale for spacing off the I = 1 and I = IMAX surfaces based upon the value of FACI1 from the initial grid binary file or the three-dimensional interpolation (default).
LREFJ		Same as above for spacing off the J = 1 and J = JMAX surfaces.
LREFK		Same as above for spacing off the K = 1 and K = KMAX surfaces.
RLXSOR		Relaxation factor for the SOR solver. Suitable values range from 0.0 to 2.0 (default = 1.0).
RLXBDE		Relaxation factor for extrapolated second derivatives at the boundary surfaces (default = 0.15).
RLXADP		Relaxation factor for grid adaptation (default = 0.15).
EPSFLD		Folding grid point criterion (default = 0.0).
EPSBAD		Sheared grid point criterion (default = sine 10°).
EPSCNV		Convergence criterion (default = 0.0001).

Namelist PBASIC

I1CONT	= 1	Control spacing and orthogonality off the I = 1 surface.
	= 0	Do not control spacing and orthogonality off the I = 1 surface (default).

IMCONT	Same as above for I = IMAX surface.
J1CONT	Same as above for J = 1 surface.
JMCONT	Same as above for J = JMAX surface.
K1CONT	Same as above for K = 1 surface.
KMCONT	Same as above for K = KMAX surface.
DELTI1	Desired spacing off the I = 1 surface. If DELTI1 = 0.0, the value will be set equal to the value of FACI1 from the initial grid binary file (default).
DELTIM	Same as above for the desired spacing off the I = IMAX surface.
DELTJ1	Same as above for the desired spacing off the J = 1 surface.
DELTJM	Same as above for the desired spacing off the J = JMAX surface.
DELTK1	Same as above for the desired spacing off the K = 1 surface.
DELTKM	Same as above for the desired spacing off the K = KMAX surface.

The following parameters control the depth of grid clustering away from the controlled surface. The default value of 0.0 produces a quasi-linear rate of spacing increase away from the boundary. Positive values produce a nonlinear rate with continuously increasing spacing in the interior. Negative values produce a nonlinear rate with near-uniform spacing in the interior.

API1	$C_{\alpha_{1,1,1}}$ for ξ_1-direction extrapolation of P_1 from I = 1 surface.
APIM	$C_{\alpha_{1,1,2}}$ for ξ_1-direction extrapolation of P_1 from I = IMAX surface.
APJ1	$C_{\alpha_{1,2,1}}$ for ξ_2-direction extrapolation of P_1 from J = 1 surface.
APJM	$C_{\alpha_{1,2,2}}$ for ξ_2-direction extrapolation of P_1 from J = JMAX surface.
APK1	$C_{\alpha_{1,3,1}}$ for ξ_3-direction extrapolation of P_1 from K = 1 surface.
APKM	$C_{\alpha_{1,3,2}}$ for ξ_3-direction extrapolation of P_1 from K = KMAX surface.
AQI1	$C_{\alpha_{2,1,1}}$ for ξ_1-direction extrapolation of P_2 from I = 1 surface.
AQIM	$C_{\alpha_{2,1,2}}$ for ξ_1-direction extrapolation of P_2 from I = IMAX surface.
AQJ1	$C_{\alpha_{2,2,1}}$ for ξ_2-direction extrapolation of P_2 from J = 1 surface.
AQJM	$C_{\alpha_{2,2,2}}$ for ξ_2-direction extrapolation of P_2 from J = JMAX surface.
AQK1	$C_{\alpha_{2,3,1}}$ for ξ_3-direction extrapolation of P_2 from K = 1 surface.
AQKM	$C_{\alpha_{2,3,2}}$ for ξ_3-direction extrapolation of P_2 from K = KMAX surface.
ARI1	$C_{\alpha_{3,1,1}}$ for ξ_1-direction extrapolation of P_3 from I = 1 surface.
ARIM	$C_{\alpha_{3,1,2}}$ for ξ_1-direction extrapolation of P_3 from I = IMAX surface.
ARJ1	$C_{\alpha_{3,2,1}}$ for ξ_2-direction extrapolation of P_3 from J = 1 surface.
ARJM	$C_{\alpha_{3,2,2}}$ for ξ_2-direction extrapolation of P_3 from J = JMAX surface.
ARK1	$C_{\alpha_{3,3,1}}$ for ξ_3-direction extrapolation of P_3 from K = 1 surface.
ARKM	$C_{\alpha_{3,3,2}}$ for ξ_3-direction extrapolation of P_3 from K = KMAX surface.

The following parameters control the depth of grid orthogonality away from the controlled boundary. Larger positive values produce increased depth (default = 3.0).

BI1	$C_{\beta_{1,1}}$ for ξ_1-direction power-law factorization of P_1, P_2, P_3 from I = 1 surface
BIM	$C_{\beta_{1,2}}$ for ξ_1-direction power-law factorization of P_1, P_2, P_3 from I = IMAX surface
BJ1	$C_{\beta_{2,1}}$ for ξ_2-direction power-law factorization of P_1, P_2, P_3 from J = 1 surface
BJM	$C_{\beta_{2,2}}$ for ξ_2-direction power-law factorization of P_1, P_2, P_3 from J = JMAX surface
BK1	$C_{\beta_{3,1}}$ for ξ_3-direction power-law factorization of P_1, P_2, P_3 from K = 1 surface
BKM	$C_{\beta_{3,2}}$ for ξ_3-direction power-law factorization of P_1, P_2, P_3 from K = KMAX surface

Namelist PADAPT

SMRATE	Rate of the penalty function for smoothness adaptation (default = 3.0). Larger values produce smoother grids tending toward the Laplacian solution.
SMORDR	Power of the penalty function for smoothness adaptation (default = 1.0). Larger values produce more smoothing near discontinuous areas.
SMBDWT	Parameter providing boundary protection for smoothness adaptation (default = 0.0).

		Larger values allow deeper penetration of the specified boundary conditions into the interior at the expense of smoothness adaptation. The maximum value of unity produces a linear penetration.
OFRNGE		Range of the penalty function for combined orthogonality and resolution adaptation, when IACCUM = 0 (default = 1.0). Larger values produce more combined adaptation. Lag of the combined orthogonality and resolution adaptation when IACCUM = 1. A zero value produces no lag, while a unity value produces full lag.
OFRATE		Rate of the penalty function for combined orthogonality and resolution adaptation. Suggested values are OFRATE = 5.0 when IACCUM = 0 and OFRATE = 50.0 when IACCUM = 1. Larger values produce more combined adaptation.
OFORDR		Power of the penalty function for combined orthogonality and resolution (default = 1.0). Larger values produce more adaptation near highly sheared and high gradient areas.
OFBDWT		Parameter providing boundary protection for combined orthogonality and resolution adaptation (default = 0.0). Larger values allow deeper penetration of the specified boundary conditions into the interior at the expense of combined adaptation. The maximum value of unity produces a linear penetration.
OTORDR		Power of the skewness function for orthogonality adaptation (default = 2.0). Larger values produce more adaptation near highly sheared areas.
WTOT		Weight factor for relative effect of orthogonality adaptation (default = 1.0).
WTFW		Weight factor for relative effect of resolution adaptation (default = 0.0).
IACCUM	= 1	Perform accumulative adaptation. The adjustments to the forcing functions are lagged, but the forcing functions always satisfy the physical constraints (default).
	= 0	Perform nonaccumulative adaptation. The adjustments to the forcing functions are immediate and are limited only by the range and rate constants.

The initial grid binary file is read from FORTRAN unit 10 with the following code:

```
      READ (10) IMAX,JMAX,KMAX
      DO 100 K=1,KMAX
      READ (10) ((X(I,J,K),I=1,IMAX),J=1,JMAX),
     *          ((Y(I,J,K),I=1,IMAX),J=1,JMAX),
     *          ((Z(I,J,K),I=1,IMAX),J=1,JMAX)
  100 CONTINUE
      READ (10) IGTYPE
      READ (10) ISING1,ISING2,ISING3,ISING4
      READ (10) JSING1,JSING2,JSING3,JSING4
      READ (10) FACI1,FACIM
      READ (10) FACJ1,FACJM
      READ (10) FACK1,FACKM
```

The variables in the binary file are defined as follows:

IMAX		Number of grid points in the ξ_1 direction.
JMAX		Number of grid points in the ξ_2 direction.
KMAX		Number of grid points in the ξ_3 direction.
X		Physical Cartesian coordinate in the x_1 direction.
Y		Physical Cartesian coordinate in the x_2 direction.
Z		Physical Cartesian coordinate in the x_3 direction.
IGTYPE	= 1	C-grid.
	= 2	H-grid.
ISING1		I-index of first line singularity on the J = 1 surface.
ISING2		I-index of second line singularity on the J = 1 surface.
ISING3		I-index of first line singularity on the J = JMAX surface.
ISING4		I-index of second line singularity on the J = JMAX surface.

JSING1	J-index of first line singularity on the I = 1 surface.
JSING2	J-index of second line singularity on the I = 1 surface.
JSING3	J-index of first line singularity on the J = JMAX surface.
JSING4	J-index of second line singularity on the J = JMAX surface.

The following values are only used if DELTI1, DELTIM, DELTJ1, DELTJM, DELTK1, and DELTKM in namelist PBASIC are defaulted.

FACI1	Desired spacing off the I = 1 surface.
FACIM	Desired spacing off the I = IMAX surface.
FACJ1	Desired spacing off the J = 1 surface.
FACJM	Desired spacing off the J = JMAX surface.
FACK1	Desired spacing off the K = 1 surface.
FACKM	Desired spacing off the K = KMAX surface.

Output from the basic solver consists of five files. The system message file is written on unit 6. The locations of any boundary and interior folding points are written on units 20 and 30, respectively. The final grid file is written on unit 40 with the same format as the initial grid file. A plot file for graphics post-processing is written on unit 50.

Folding points are identified where the normalized Jacobian is negative. Sheared points are identified where the normalized Jacobian is less than EPSBAD. An error index is computed every ten iterations and is defined as the relative movement of a point normalized by the diagonal length of the grid. Convergence is attained when the absolute maximum error index among all points is less than EPSCNV with no folding points.

APPENDIX B

USER'S MANUAL FOR GEOMETRY PREPROCESSOR

The preprocessor is coded in FORTRAN IV as program BLADE with 39 subprograms. A two-dimensional version of the basic solver is included as subroutine GRID2D to define nodal point distributions on the hub and shroud boundary surfaces. The nonstandard PARAMETER statement is used to facilitate dimensioning of arrays, while the nonstandard NAMELIST feature is used for quasi-free-format input.

Input to the preprocessor comprises three namelists read on unit 5 for GRID2D, one namelist read on unit 7 for BLADE, and formatted blade geometry data on unit 8. The type (REAL or INTEGER) of each variable follows standard FORTRAN convention. The I, J, and K indices correspond to the ξ_1, ξ_2, and ξ_3 directions, respectively.

Namelist SYSTEM (Unit 5)

ISYS	= 1	Solve governing equation as a Laplacian system without forcing functions (default). This option produces a grid that tends toward uniform spacing away from curved boundaries, but produces smaller spacing near convex boundaries and larger spacing near concave boundaries.
	= 2	Solve governing equation as a Poission system with forcing functions. This option allows specificaton of spacing and orthogonality at the boundaries.
ICHECK	= 1	Check boundary structures for grid folding and write report on unit 20.
	= 0	Bypass boundary structure check (default).
ICONT	= 0	Terminate operation if boundary structure grid folding is detected.
	= 1	Continue operation (default).
ITMAX		Maximum number of overall iterations (default = 100).
RLXSOR		Relaxation factor for the SOR solver. Suitable values range from 0.0 to 2.0 (default = 1.0).
RLXBDE		Relaxation factor for extrapolated second derivatives at the boundary surfaces (default = 0.15).
RLXADP		Relaxation factor for grid adaptation (default = 0.15).
EPSFLD		Folding grid point criterion (default = 0.0).
EPSBAD		Sheared grid point criterion (default = sine 10°).
EPSCNV		Convergence criterion (default = 0.0001).

Namelist PBASIC (Unit 5)

I1CONT	= 1	Control spacing and orthogonality off the I =1 surface.
	= 0	Do not control spacing and orthogonality off the I = 1 surface (default).
IMCONT		Same as above for I = IMAX surface.
J1CONT		Same as above for J = 1 surface.
JMCONT		Same as above for J = JMAX surface.
DELTI1		Desired spacing off the I = 1 surface. If DELTI1 = 0.0, the value will be set equal to the value of FACI1 from the initial grid binary file (default).
DELTIM		Same as above for the desired spacing off the I = IMAX surface.
DELTJ1		Same as above for the desired spacing off the J = 1 surface.
DELTJM		Same as above for the desired spacing off the J = JMAX surface.

The following parameters control the depth of grid clustering away from the controlled surface. The default value of 0.0 produces a quasi-linear rate of spacing increase away from the boundary. Positive values produce a nonlinear rate with continuously increasing spacing in the interior. Negative values produce a nonlinear rate with near-uniform spacing in the interior.

API1	$C_{\alpha_{1,1,1}}$ for ξ_1-direction extrapolation of P_1 from I = 1 surface.
APIM	$C_{\alpha_{1,1,2}}$ for ξ_1-direction extrapolation of P_1 from I = IMAX surface.
APJ1	$C_{\alpha_{1,2,1}}$ for ξ_2-direction extrapolation of P_1 from J = 1 surface.
APJM	$C_{\alpha_{1,2,2}}$ for ξ_2-direction extrapolation of P_1 from J = JMAX surface.
AQI1	$C_{\alpha_{2,1,1}}$ for ξ_1-direction extrapolation of P_2 from I = 1 surface.
AQIM	$C_{\alpha_{2,1,2}}$ for ξ_1-direction extrapolation of P_2 from I = IMAX surface.
AQJ1	$C_{\alpha_{2,2,1}}$ for ξ_2-direction extrapolation of P_2 from J = 1 surface.
AQJM	$C_{\alpha_{2,2,2}}$ for ξ_2-direction extrapolation of P_2 from J = JMAX surface.

The following parameters control the depth of grid orthogonality away from the controlled boundary. Larger positive values produce increased depth (default = 3.0).

BI1	$C_{\beta_{1,1}}$ for ξ_1-direction power-law factorization of P_1 and P_2 from I = 1 surface
BIM	$C_{\beta_{1,2}}$ for ξ_1-direction power-law factorization of P_1 and P_2 from I = IMAX surface
BJ1	$C_{\beta_{2,1}}$ for ξ_2-direction power-law factorization of P_1 and P_2 from J = 1 surface
BJM	$C_{\beta_{2,2}}$ for ξ_2-direction power-law factorization of P_1 and P_2 from J = JMAX surface

Namelist PADAPT (Unit 5)

SMRATE		Rate of the penalty function for smoothness adaptation (default = 3.0). Larger values produce smoother grids tending toward the Laplacian solution.
SMORDR		Power of the penalty function for smoothness adaptation (default = 1.0). Larger values produce more smoothing near discontinuous areas.
SMBDWT		Parameter providing boundary protection for smoothness adaptation (default = 0.0). Larger values allow deeper penetration of the specified boundary conditions into the interior at the expense of smoothness adaptation. The maximum value of unity produces a linear penetration.
OFRNGE		Range of the penalty function for combined orthogonality and resolution adaptation, when IACCUM = 0 (default = 1.0). Larger values produce more combined adaptation. Lag of the combined orthogonality and resolution adaptation when IACCUM = 1. A zero value produces no lag, while a unity value produces full lag.
OFRATE		Rate of the penalty function for combined orthogonality and resolution adaptation. Suggested values are OFRATE = 5.0 when IACCUM = 0 and OFRATE = 50.0 when IACCUM = 1. Larger values produce more combined adaptation.
OFORDR		Power of the penalty function for combined orthogonality and resolution (default = 1.0). Larger values produce more adaptation near highly sheared and high gradient areas.
OFBDWT		Parameter providing boundary protection for combined orthogonality and resolution adaptation (default = 0.0). Larger values allow deeper penetration of the specified boundary conditions into the interior at the expense of combined adaptation. The maximum value of unity produces a linear penetration.
OTORDR		Power of the skewness function for orthogonality adaptation (default = 2.0). Larger values produce more adaptation near highly sheared areas.
WTOT		Weight factor for relative effect of orthogonality adaptation (default = 1.0).
WTFW		Weight factor for relative effect of resolution adaptation (default = 0.0).
IACCUM	= 1	Perform accumulative adaptation. The adjustments to the forcing functions are lagged, but the forcing functions always satisfy the physical constraints (default).
	= 0	Perform nonaccumulative adaptation. The adjustments to the forcing functions are immediate and are limited only by the range and rate constants.

Namelist BLDATA (Unit 7)

IGTYPE	= 1	Generate C-grid.
	= 2	Generate H-grid.
DELTAT		Periodic pitch angle in radians.

KCUT	Number of blade geometry cuts in the K-direction supplied on unit 8.
KMAX	Desired number of grid points in the K-direction.
FACK1	Desired spacing off the K = 1 surface.
FACK2	Desired spacing off the K = KMAX surface.
PWK	Power of stretching function for the K-direction (default = 1.0). Larger values produce tighter clustering near the boundaries.
NBLD	Desired number of points on upper and lower blade surfaces.
FACB1	Desired spacing on the blade at leading edge.
FACB2	Desired spacing on the blade at trailing edge.
PWBD	Power of stretching function for the blade point distribution (default = 1.0). Larger values produce tighter clustering at the boundaries.
NLEAD	Desired number of points on the leading edge branch cut (H-grid only).
FLCUT1	Desired spacing on leading edge branch cut at leading edge (H-grid only). If FLCUT1 > 100.0, the spacing on the branch cut at the leading edge will match the spacing on the blade at the leading edge.
FLCUT2	Desired spacing on leading edge branch cut at inlet (H-grid only).
NTAIL	Desired number of points on trailing edge branch cut.
FTCUT1	Desired spacing on trailing edge branch cut at trailing edge. If FTCUT1 > 100.0, the spacing on the branch cut at the trailing edge will match the spacing on the blade at the trailing edge.
FTCUT2	Desired spacing on trailing edge branch cut at outlet.
PWCUT	Power of stretching function for the branch cut point distributions (default = 1.0). Larger values produce tighter clustering at the boundaries.
NIO	Desired number of points in the J-direction at the outlet from trailing edge branch cut to the periodic lines for C-grid or one-half the desired number of points in the J-direction at the inlet and outlet for H-grid.
FACIO1	Desired spacing in the J-direction off the branch cut at the outlet for C-grid or desired spacing in the J-direction off the periodic surfaces at the inlet and outlet for H-grid.
FACIO2	Desired spacing in the J-direction off the periodic surfaces at the outlet for C-grid or desired spacing in the J-direction at the center of the inlet and outlet for H-grid.

The following parameters apply only to the C-grid:

ISL	Desired number of points on lower half of inlet section.
ISU	Desired number of points on upper half of inlet section.
FPDA	Desired spacing at center of inlet section.
FPDB	Desired spacing at edges of inlet section.
PWIN	Power of stretching function for inlet section point distribution (default = 1.0). Larger values produce tighter clustering at the boundaries.
FPDC	Desired spacing on the periodic surfaces at the inlet.
FPDD	Desired spacing on the periodic surfaces at the outlet.
PWPRD	Power of stretching function for point distribution on the periodic surfaces (default = 1.0). Larger values produce tighter clustering at the boundaries.

The formatted blade geometry data is read from FORTRAN unit 8 with the following code:

```
DO 680 K=1,KCUT
READ (8,1010) NPATH
READ (8,1020) (ZPATH(I),I=1,NPATH)
READ (8,1020) (RPATH(I),I=1,NPATH)
READ (8,1010) IBLDP
READ (8,1020) (BLDPZC(I),I=1,IBLDP)
READ (8,1020) (BLDPTC(I),I=1,IBLDP)
```

```
      READ (8,1020) (BLDPRC(I),I=1,IBLDP)
      READ (8,1010) IBLDS
      READ (8,1020) (BLDSZC(I),I=1,IBLDS)
      READ (8,1020) (BLDSTC(I),I=1,IBLDS)
      READ (8,1020) (BLDSRC(I),I=1,IBLDS)
      READ (8,1020) SLOPL,SLOPT
      .
      .
      .
  680 CONTINUE
      .
      .
      .
 1010 FORMAT (1I3)
 1020 FORMAT (8F10.0)
```

The variables in the formatted file are defined as follows:

NPATH	Total number of data points defining the surface cut.
ZPATH	Axial coordinates of data points on the surface cut.
RPATH	Radial coordinates of data points on the surface cut.
IBLDP	Total number of data points defining the pressure or lower surface of blade.
BLDPZC	Axial coordinates of data points on pressure surface.
BLDPTC	Circumferential coordinates of data points on pressure surface (in radians).
BLDPRC	Radial coordinates of data points on pressure surface.
IBLDS	Total number of data points defining the suction or upper surface of blade.
BLDSZC	Axial coordinates of data points on suction surface.
BLDSTC	Circumferential coordinates of data points on suction surface (in radians).
BLDSRC	Radial coordinates of data points on suction surface.
SLOPL	Tangent of inflow angle or leading edge mean camber angle. If SLOPL > 100.0, SLOPL will be reset to match the computed leading edge mean camber angle.
SLOPT	Tangent of outflow angle or trailing edge mean camber angle. If SLOPT > 100.0, SLOPT will be reset to match the computed trailing edge mean camber angle.

Output from the preprocessor consists of eight files. The system message file is written on unit 6. The initial grid file is written on unit 10 for use by the basic solver. The locations of any boundary folding points on the hub and shroud surfaces are written unit 20. The location of any interior folding points on the hub and shroud surfaces are written on unit 30. The computed nodal point distributions for the hub and shroud surfaces are written on units 40 and 45. Plot files for graphics post-processing are written on units 50 and 55 for the hub and shroud surfaces.

Folding points are identified where the normalized Jacobian is negative. Sheared points are identified where the normalized Jacobian is less than EPSBAD. An error index is computed every ten iterations and is defined as the relative movement of a point normalized by the diagonal length of the grid. Convergence is attained when the absolute maximum error index among all points is less than EPSCNV with no folding points.

The initial grid binary file is written on FORTRAN unit 10 with the following code:

```
      WRITE (10) IMAX,JMAX,KMAX
      DO 100 K=1,KMAX
      WRITE (10) ((X(I,J,K),I=1,IMAX),J=1,JMAX),
     *           ((Y(I,J,K),I=1,IMAX),J=1,JMAX),
     *           ((Z(I,J,K),I=1,IMAX),J=1,JMAX)
  100 CONTINUE
```

```
WRITE (10) IGTYPE
WRITE (10) ISING1,ISING2,ISING3,ISING4
WRITE (10) JSING1,JSING2,JSING3,JSING4
WRITE (10) FACI1,FACIM
WRITE (10) FACJ1,FACJM
WRITE (10) FACK1,FACKM
```

The variables in the binary file are defined as follows:

IMAX		Number of grid points in the ξ_1 direction.
JMAX		Number of grid points in the ξ_2 direction.
KMAX		Number of grid points in the ξ_3 direction.
X		Physical Cartesian coordinate in the x_1 direction.
Y		Physical Cartesian coordinate in the x_2 direction.
Z		Physical Cartesian coordinate in the x_3 direction.
IGTYPE	= 1	C-grid.
	= 2	H-grid.
ISING1		I-index of first line singularity on the J = 1 surface.
ISING2		I-index of second line singularity on the J = 1 surface.
ISING3		I-index of first line singularity on the J = JMAX surface.
ISING4		I-index of second line singularity on the J = JMAX surface.
JSING1		J-index of first line singularity on the I = 1 surface.
JSING2		J-index of second line singularity on the I = 1 surface.
JSING3		J-index of first line singularity on the J = JMAX surface.
JSING4		J-index of second line singularity on the J = JMAX surface.
FACI1		Desired spacing off the I = 1 surface.
FACIM		Desired spacing off the I = IMAX surface.
FACJ1		Desired spacing off the J = 1 surface.
FACJM		Desired spacing off the J = JMAX surface.
FACK1		Desired spacing off the K = 1 surface.
FACKM		Desired spacing off the K = KMAX surface.

REFERENCES

1. Thompson, Joe F.; Warsi, Z. U. A.; and Marstin, C. Wayne: Numerical Grid Generation: Foundations and Applications. Elsevier Science Publishing Co., 1985.

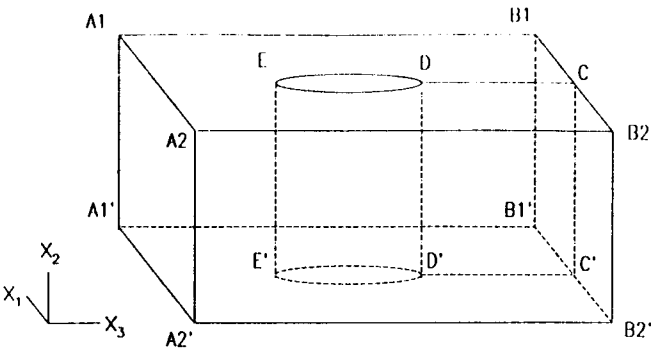

(A) C-GRID IN PHYSICAL SPACE.

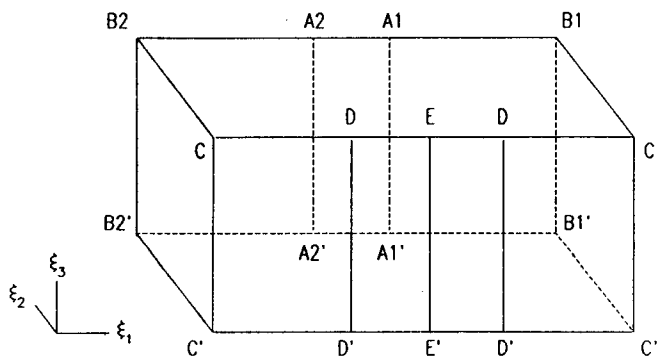

(B) C-GRID IN COMPUTATIONAL SPACE.

FIGURE 1. - C-GRID ABOUT GENERIC BLADE.

ORIGINAL PAGE IS
OF POOR QUALITY

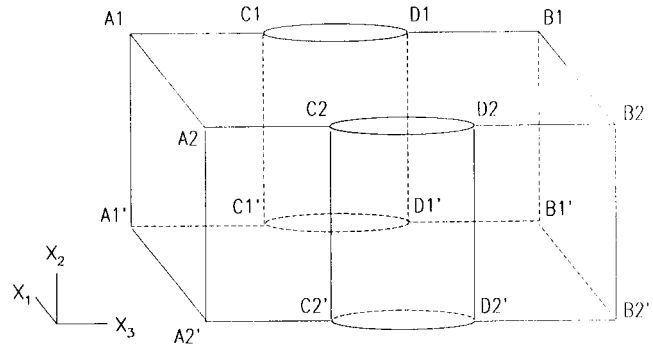

(A) H-GRID IN PHYSICAL SPACE.

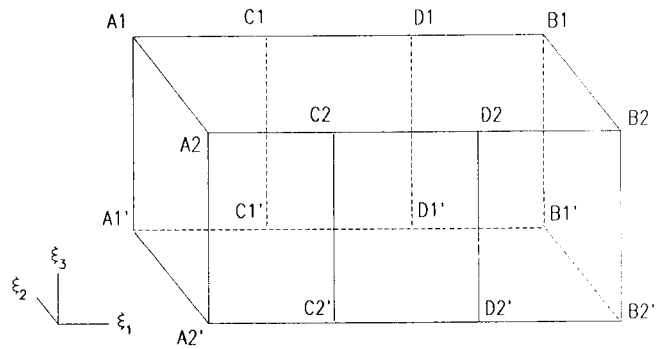

(B) H-GRID IN COMPUTATIONAL SPACE.

FIGURE 2. - H-GRID BETWEEN GENERIC BLADES.

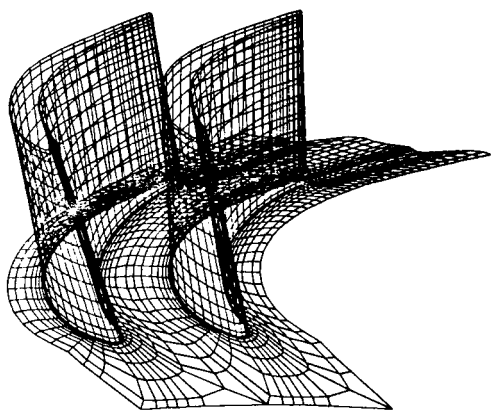

FIGURE 3. - THREE-DIMENSIONAL C-GRID FOR TURBINE ROTOR.

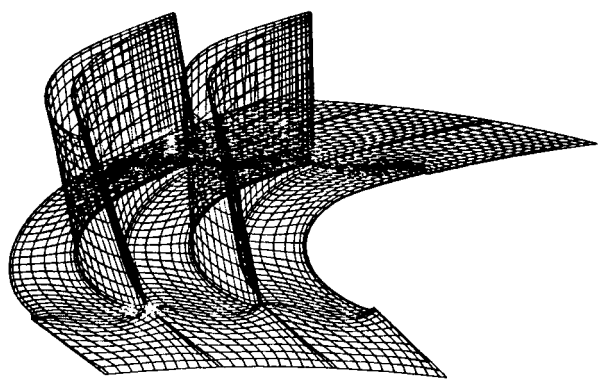

FIGURE 4. - THREE-DIMENSIONAL H-GRID FOR TURBINE ROTOR.

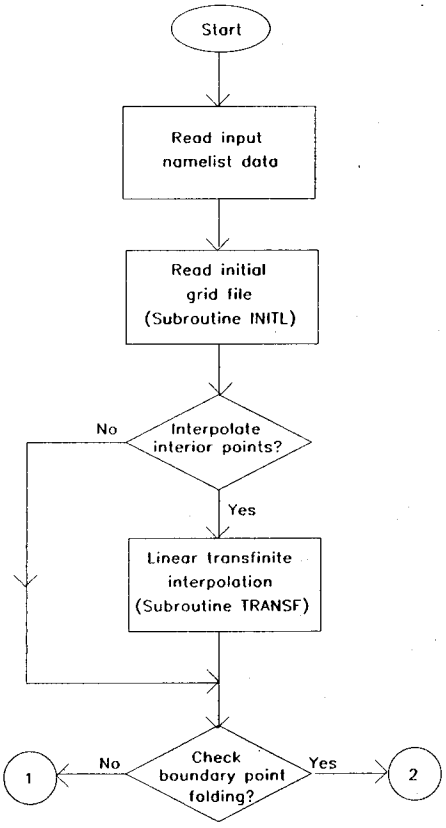

FIGURE 5. - FLOW CHART FOR PROGRAM GRID 3D.

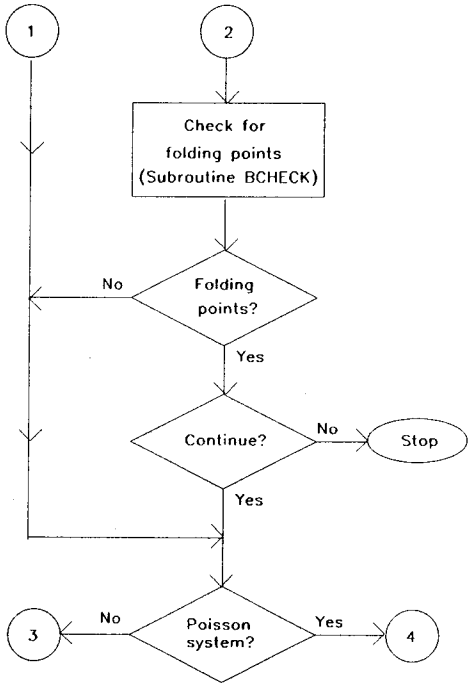

FIGURE 5. - CONTINUED.

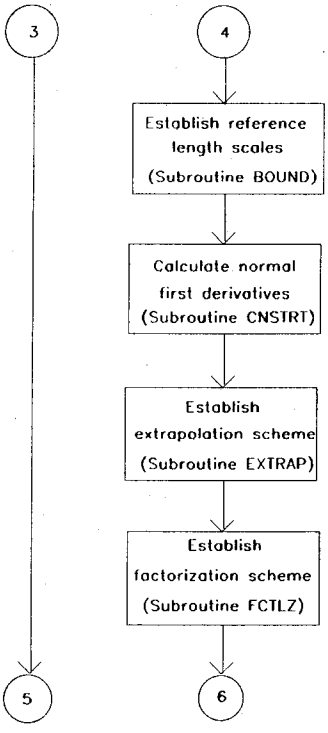

FIGURE 5. - CONTINUED.

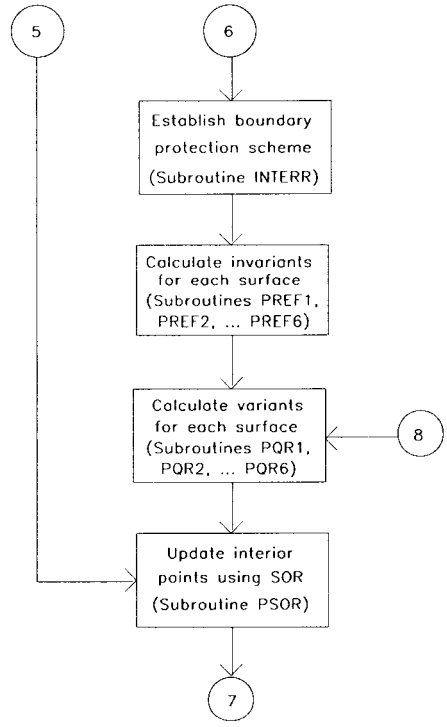

FIGURE 5. - CONTINUED.

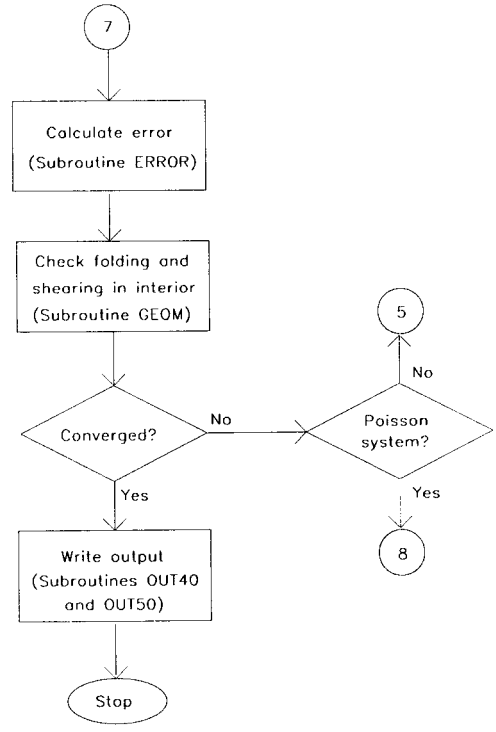

FIGURE 5. - CONCLUDED.

NASA
National Aeronautics and Space Administration

Report Documentation Page

1. Report No.	2. Government Accession No.	3. Recipient's Catalog No.
NASA TM-101330		

4. Title and Subtitle

Three-Dimensional Elliptic Grid Generation Technique With Application to Turbomachinery Cascades

5. Report Date

August 1988

6. Performing Organization Code

7. Author(s)

S.C. Chen and J.R. Schwab

8. Performing Organization Report No.

E-4342

10. Work Unit No.

582-01-11

9. Performing Organization Name and Address

National Aeronautics and Space Administration
Lewis Research Center
Cleveland, Ohio 44135-3191

11. Contract or Grant No.

13. Type of Report and Period Covered

Technical Memorandum

12. Sponsoring Agency Name and Address

National Aeronautics and Space Administration
Washington, D.C. 20546-0001

14. Sponsoring Agency Code

15. Supplementary Notes

S.C. Chen, Sverdrup Technology, Inc., NASA Lewis Research Center Group, Cleveland, Ohio 44135; J.R. Schwab, NASA Lewis Research Center.

16. Abstract

This report describes a numerical method for generating three-dimensional grids for turbomachinery computational fluid dynamics codes. The basic method is general and involves the solution of a quasi-linear elliptic partial differential equation via pointwise relaxation with a local relaxation factor. It allows specification of the grid point distribution on the boundary surfaces, the grid spacing off the boundary surfaces, and the grid orthogonality at the boundary surfaces. It includes adaptive mechanisms to improve smoothness, orthogonality, and flow resolution in the grid interior. A geometry preprocessor constructs the grid point distributions on the boundary surfaces for general turbomachinery cascades. Representative results are shown for a C-grid and an H-grid for a turbine rotor. Two appendices serve as user's manuals for the basic solver and the geometry preprocessor.

17. Key Words (Suggested by Author(s))	18. Distribution Statement
Grid generation Turbomachinery	Unclassified – Unlimited Subject Category 34

19. Security Classif. (of this report)	20. Security Classif. (of this page)	21. No of pages	22. Price*
Unclassified	Unclassified	20	A03

*For sale by the National Technical Information Service, Springfield, Virginia 22161